Fixed-time Adaptive Neural Control for Robot Manipulators with Input Saturation and Disturbance

Haiqi Huang[1], Zhenyu Lu[2], Ning Wang[2], Chenguang Yang[2]

***Abstract*—A fixed-time adaptive neural network control scheme is designed for an unknown model manipulator system with input saturation and external environment disturbance, so that the system convergence time can be parameterized and not affected by the initial state of the system. The compensation control item is introduced to compensate for external disturbance. The scheme can ensure that the input torque always does not exceed the actuator saturation value and the transient and steady state performance will not significantly degrade. Furthermore, the Incremental Broad Neural Network (IBNN) is used for approximating unknown models with flexible adjustability and high computational efficiency, so it can be applied to scenarios with different control precision requirements. Simulation results verify the effectiveness of the scheme in the above aspects.**

***Index Terms*—input saturation, manipulator, fixed-time control, Incremental Broad Neural Network**

I. Introduction

Convergence time is a vital evaluating indicator of the control system. In nonlinear systems, the finite time control theory is first proposed, which creatively parameterizes the upper limit of convergence time of nonlinear systems and can adjust the convergence time through parameter design [1], [2]. However, it also has some limitations such as the upper bound of the convergence time that will be affected by the initial state of the system. Unfortunately, in practical application scenarios, the initial state of the system is often random and cannot be adjusted to the ideal state as the designer wished. Therefore, the convergence time of the scheme based on finite time stable control is still unknown in many cases. Therefore, for solving the above limitation, fixed time stability theory [3] was then proposed with the advantage of making the upper bound of convergence time independent of the initial state of the system [4]. Thus, it can get a better convergence time by adjusting the parameters, making it more suitable for practical system design. In recent years, this theory has developed rapidly and many excellent research results have emerged in [5]–[9].

In the field of robot manipulator control, neural network is an important tool for modeling nonlinear complex systems. Neural network has a strong nonlinear mapping ability and can build the model of an unknown system through its known system input and output signals. The approximation performance of the neural network depends on if the input vector is included in the compact set domain of the neural network. However, the nodes of the traditional neural network need to be set up in advance, which requires certain prior knowledge [10], [11]. Once the nodes are set up improperly, the performance of NN will deteriorate. In the neural network controller, when the approximation performance of the neural network cannot meet the requirements of control accuracy, the common approach will increase the number of layers and nodes of the neural network. However, in the traditional neural network [12], [13], the weights of the network needs to be retrained, and the computational efficiency will be reduced, making it difficult to ensure real-time performance.

Due to the limitations of its physical properties, there is always an upper limit for the input that can be accepted by the manipulator actuator in the real scene, which is also the maximum torque that can be input when we design the controller. However, the ideal input saturation curve is a big challenge to controller design, because the curve is not differentiable at two inflection points, and the control signals do not change smoothly, which is not feasible. Therefore, in practical design, the saturation effect function used to assist the design needs to select smooth function, such as "$\tanh(\cdot)$" function [9], [14], [15] and "$\arctan(\cdot)$" function [16]. Meanwhile, due to the complexity of the working environment, the manipulator is usually affected by external disturbances during operation, and the performance of the control system declines if the disturbance is not compensated in the controller design.

Inspired by the above situations, we propose a fixed-time neural network control scheme with the four contributions as follows:

1) The tracking error of the system converges to a stable state within the fixed time, and the tangent convergence time is independent of the initial state.

2) The control law conversion is designed so that the system can handle saturation effect and the torque in the whole tracking process is ensured to keep within the saturation value.

3) For the disturbance torque of the external environment, a compensation term is designed to increase the robustness of the system.

4) The Incremental Broad Neural Network (IBNN) is designed and used to approximate the unknown system model, which has flexible adjustability and high computational efficiency under different control performance requirements.

This work was partially supported by the H2020 Marie Sklodowska-Curie Actions Individual Fellowship under Grant 101030691.

[1] H. Huang is with College of Automation Science and Engineering, South China University of Technology, Guangzhou 510640, China

[2]Z. Lu, N. Wang and C. Yang are with Bristol Robotics Laboratory, University of the West of England, Bristol, BS16 1QY, UK.

Corresponding author is C. Yang. (Email: cyang@ieee.org)

II. System Model

The dynamic equation of manipulators with n degrees of robot freedom (DOF) can be represented as:

$$H\ddot{\theta} + C\dot{\theta} + G + \tau_{dist} = \tau \tag{1}$$

where $\theta \in \mathbb{R}^n$ is the joint angle , $H \in \mathbb{R}^{n\times n}$ is the inertia matrix, $C \in \mathbb{R}^{n\times n}$ is the Corianis matrix, $G \in \mathbb{R}^n$ represents the gravity, $\tau_{dist} \in \mathbb{R}^n$ represents external disturbance, $\tau \in \mathbb{R}^n$ represents the control moment. The robot manipulator has the following two commonly used properties:

Propert 1: For any θ,$\dot{\theta} \in \mathbb{R}^n$, H, C, G are all bounded and their first-order can guide.

Propert 2: $\dot{H} - 2C$ is an antisymmetric matrix, that is, for any $z \in \mathbb{R}^n$, $z^T(\dot{H} - 2C)z = 0$ are established.

III. Preliminaries

A. Incremental Broad Neural Network (IBNN)

Broad Neural Network (BNN) [17] is an optimization improvement based on the Random Vector Functional-link Neural Networks(RVFLNN) [18].

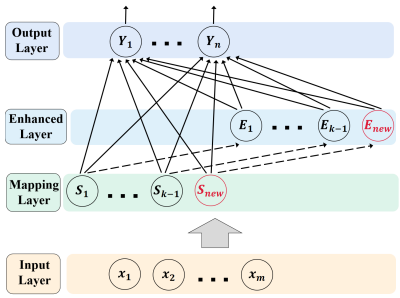

Fig. 1: Structure of Incremental Broad Neural Network.

For the purpose of making the node distribution of neural network more reasonable, we introduce the Incremental Broad Neural Network (IBNN) into the controller, whose structure is shown in Figure 1. Its expression is

$$Y_i(x) = W_i^T\Phi(x) + \epsilon_i(x),\ \ i = 1, 2, \ldots, n \tag{2}$$

where $\epsilon_i(x)$ is the approximation error, $\Phi(x) \in \mathbb{R}^{3k}$ is the generalized feature mapping layer composed of mapping layer and enhancement layer, i.e

$$\Phi(x) = [S_1(x), ..., S_{new}(x), E_1(x), ..., E_{new}(x)]^T \tag{3}$$

where each $S_i(x), i = 1, 2, \ldots, k$ corresponds to a neural network node, $S_k(x) = S_{new}(x)$ indicates that the k^{th} node is latest generated node generated by the incremental learning [19]. The principle of incremental learning is to intelligently generate network nodes according to the system input ,ensuring that the input is always in the compact set domain. $S_i(x)$ represents the feature mapping function, which is chosen as a Gaussian function:

$$S_i(x) = exp[\frac{-(x-\mu_i)^T(x-\mu_i)}{\sigma_i^2}],\ \ i = 1, \ldots, k \tag{4}$$

where $x = [x_1, x_2, \ldots, x_m]^T$ is input vector, $\mu_i \in \mathbb{R}^m$ denotes the i^{th} node, σ_i is its corresponding width. $E_i(x) \in \mathbb{R}^{1\times 2}$ in (3) represents the enhancement layer which is generated by extracting the effective information of the mapping layer. Here, we use a trigonometric function:

$$E_i(x) = [sin(S_i(x)), cos(S_i(x))],\ \ i = 1, \ldots, k \tag{5}$$

B. Lemmas and remarks

Lemma 1 [20]: For a positive definite Lyapunov function $V(x)$, if its initial state $V(x_0)$ is bounded, it is first-order derivable under any value of x, and its deivative satisfies the inequality:$\dot{V} < -pV + q$, $p > 0$, $q > 0$, then the system signals are uniformly ultimately bounded(UUB).

Lemma 2 [10]: For a positive definite Lyapunov function $V(x)$, if it holds: $\dot{V} < -pV^\alpha - qV^\beta + h$, $p > 0$, $q > 0$, $h > 0, 0 < \alpha < 1, \beta > 1$, then the system $\dot{x} = f(x, t)$ is fixed-time stable, and its solution will converges to a compact set $\Omega = \left\{x|V \le min\left([h/(p(1-\gamma))]^{1/\alpha}, [h/(q(1-\gamma))]^{1/\beta}\right)\right\}$, where $0 < \gamma < 1$. Besides, the convergence time of the system satisfies: $T \le T_{max} = \frac{1}{p\gamma(1-\alpha)} + \frac{1}{q\gamma(\beta-1)}$.

Lemma 3 [21]: For any scalar a_i, we have

$$\sum_{i=1}^{n}|a_i|^r \ge \left(\sum_{i=1}^{n}|a_i|\right)^r, \quad 0 < r \le 1 \tag{6}$$

$$\sum_{i=1}^{n}|a_i|^r \ge n^{1-r}\left(\sum_{a=1}^{n}|a_i|\right)^r, \quad r > 1 \tag{7}$$

Definition 1 : We define the "$Sig^r(\cdot)$" and "$Sgn(\cdot)$" function

$$\begin{aligned} Sig^r(x) &= [|x_1|^r sign(x_1), ..., |x_n|^r sign(x_n)]^T \\ Sgn(x) &= [sign(x_1), ..., sign(x_n)]^T \end{aligned} \tag{8}$$

where $x = [x_1, x2, ..., x_n], i = 1, ..., n$, r is a positive constant, while $sign(\cdot)$ is signum function.

Definition 2 : We define the "$\odot$" operation as follows:

$$x \odot y = [x_1y_1, ..., x_ny_n]^T \tag{9}$$

wher $x = [x_1, ..., x_n]^T$, $y = [y_1, ..., y_n]^T$.

IV. Controller Design

A. Fixed-time controller

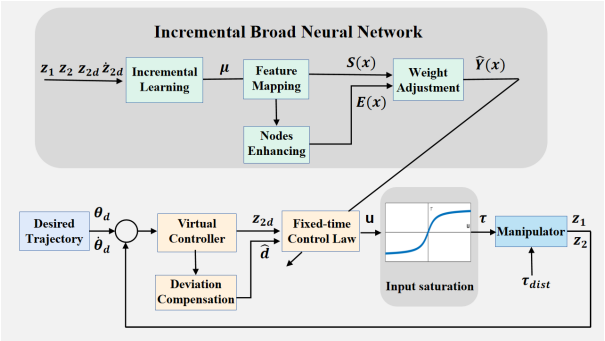

Fig. 2: Fixed-time IBNN Tracking Control Scheme.

We set $z_1 = \theta$, $z_2 = \dot{\theta}$ as the state variables. According to (1), the state space equation of the manipulator can be sorted out as:

$$\begin{cases} \dot{z}_1 = z_2 \\ \dot{z}_2 = H^{-1}(\tau - Cz_2 - G - \tau_{dist}) \end{cases} \tag{10}$$

The error signal can be obtained as:

$$\begin{cases} \tilde{z}_1 = z_1 - \theta_d \\ \tilde{z}_2 = z_2 - z_{2d} \end{cases} \tag{11}$$

where $\theta_d \in \mathbb{R}^n$ is the desired value, and $z_{2d} \in \mathbb{R}^n$ is the virtual control law that is designed in subsequent process.

The error dynamic equation can be obtained as:

$$H\dot{\tilde{z}}_2 + C\tilde{z}_2 = \tau - H\dot{z}_{2d} - Cz_{2d} - G - \tau_{dist} \tag{12}$$

According to the backstepping control method, the virtual control law z_{2d} is designed as:

$$z_{2d} = -K_{11}\tilde{z}_1 - K_{12}Sig^{\alpha}(\tilde{z}_1) - K_{13}Sig^{\beta}(\tilde{z}_1) + \dot{\theta}_d \tag{13}$$

where K_{11}, K_{12}, $K_{13} \in \mathbb{R}^{n\times n}$ are diagonal matrices with positive elements, $0 < \alpha < 1$, $\beta > 1$.

In order to make the network have flexibility of adjustment and high computational efficiency under different approximation performance requirements, we adopt the Incremental Broad Neural Network mentioned above to estimate the uncertain model of the system, i.e.,

$$Y(x) = -H\dot{z}_{2d} - Cz_{2d} - G = W^T\Phi(x) + \epsilon(x) \tag{14}$$

where $x = [z_1^T, z_2^T, z_{2d}^T, \dot{z}_{2d}^T]$, $\epsilon(x)$ is the approximation error of the network.

In order to address the input saturation problem, we need to introduce an auxiliary diagonal matrix Υ:

$$\Upsilon = diag[\frac{\bar{\tau}_i}{\bar{u}_i}] \ , i = 1, 2, \ldots, n \tag{15}$$

where $\bar{\tau}_i$ denotes the i^{th} joint actuator saturation value, which means$|\tau_i| \leq \bar{\tau}_i$, $\bar{u}_i$ is related to the expected maximum control law in the design of controller parameters.

The derivative of $\tilde{z}_2$ with respect to time is

$$\dot{\tilde{z}}_2 = \dot{z}_2 - \dot{z_{2d}} = H^{-1}(\Upsilon\Upsilon^{-1}\tau + Y(x) - \tau_{dist}) - H^{-1}C\tilde{z} \tag{16}$$

The relation between the real control torque τ and the designed control law u is as follows:

$$\tau = s(u) + \Delta\tau \tag{17}$$

where $\Delta\tau$ represents the difference between the reakl value and the desired value of the input saturatione. $s(u) \in \mathbb{R}^n$ represents the conversion value of the control law $u \in \mathbb{R}^n$ after saturation effect, which is also the actual input to the controller. Here we use the "$arctan(\cdot)$" function to handle the input saturation, i.e

$$s_i(u) = \frac{\bar{\tau}_i}{\omega_i} arctan(\frac{\omega_i u_i}{\bar{u}_i}) \ , i = 1, 2, \ldots, n \tag{18}$$

where $\omega_i = \pi/2$. According to [16], the following equation holds

$$\Upsilon^{-1}s(u) = \chi(u)u \tag{19}$$

$$\chi(u) = diag[\frac{1}{1 + (\eta_i\omega_i u_i/\bar{u}_i)^2}] \ , i = 1, 2, \ldots, n \tag{20}$$

where $0 < \eta_i < 1$. Thus (16) can be rewritten as:

$$\dot{\tilde{z}}_2 = H^{-1}(\Upsilon\chi(u)u + \Delta\tau + W^T\Phi(x) + \epsilon - \tau_{dist}) - H^{-1}C\tilde{z} \tag{21}$$

Due to the uncertain deviation terms such as torque disturbance τ_{dist} and error $\Delta\tau + \epsilon$ in (21), it is necessary to compensate these bounded error terms in real systems, and we assume its upper bound as

$$\Delta\tau_i + \epsilon_i - \tau_{dist,i} \leq \sum_{i=1}^{n}(sup(|\Delta\tau_i| + |\epsilon_i| + |\tau_{dist,i}|)) = d_i \tag{22}$$

where $sup(\cdot)$ indicates the upper bound.$\hat{d}$ represents the estimated value of d, and the estimated error $\tilde{d}$ is defined as:

$$\tilde{d} = d - \hat{d} \tag{23}$$

Meanwhile, the update law of $\hat{d}$ is

$$\dot{\hat{d}} = Sgn(\tilde{z}_2) \odot \tilde{z}_2 - \upsilon\hat{d} \tag{24}$$

According to the saturation effect and fixed time stability theory, we designed the original control law u as follows:

$$u = \Upsilon^{-1}u_a \tag{25}$$

$$\begin{aligned} u_a = &- z_1 - K_{21}\tilde{z}_2 - K_{22}Sig^{\alpha}(\tilde{z}_2) - K_{23}Sig^{\beta}(\tilde{z}_2) \\ &- \hat{W}^T\Phi(x) - Sgn(\tilde{z}_2) \odot \hat{d} \end{aligned} \tag{26}$$

where K_{21}, K_{22}, K_{23} are all diagonal matrices, and $\hat{W}$ is the estimate of the weight W of the neural network. Here we define the estimation error $\tilde{W} = W - \hat{W}$. Finally, we design a new law for the weights of neural networks

$$\dot{\hat{W}} = \Gamma(\Phi(x)\tilde{z}_2^T - \lambda\hat{W}) \tag{27}$$

where $\Gamma \in \mathbb{R}^{k\times k}$,$\lambda \in \mathbb{R}^{k\times k}$ are both diagonal matrices, whose elements are positive constants.

B. Stability Analysis

This part will be performed in two steps. The first step is to prove that the whole system is Lyapunov stable, thus that some error signals are bounded for the convenience of the second part of the proof. The second step is to prove that the position tracking error of the manipulator converges in fixed time on the premise of the first step.

We first build three regularization equations using the error terms $\tilde{z}_1$, $\tilde{z}_2$,$\tilde{d}$, $\tilde{W}$:

$$\begin{aligned} V_1 =& \frac{1}{2}\tilde{z}_1^T\tilde{z}_1 \\ V_2 =& \frac{1}{2}\tilde{z}_2^T H\tilde{z}_2 \\ V_3 =& \frac{1}{2}\tilde{d}^T\tilde{d} + \frac{1}{2}tr(\tilde{W}^T\Gamma^{-1}\tilde{W}) \end{aligned} \tag{28}$$

Combining (10), (12) and (13), we can acquire $\dot{V}_1$ as

$$\begin{aligned}\dot{V}_1 =&\tilde{z}_1^T\dot{\tilde{z}}_1\\ =&\tilde{z}_1^T(\tilde{z}_2 - K_{11}\tilde{z}_1 - K_{12}Sig^{\alpha}(\tilde{z}_1) - K_{13}Sig^{\beta}(\tilde{z}_1))\\ =&\tilde{z}_1^T\tilde{z}_2 - \sum_{i=1}^{n}(k_{11,i}\tilde{z}_{1,i}^2) - \sum_{i=1}^{n}(k_{12,i}|\tilde{z}_{1,i}|^{\alpha+1})\\ &- \sum_{i=1}^{n}(k_{13,i}|\tilde{z}_{1,i}|^{\beta+1})\end{aligned} \tag{29}$$

Combining (20), (21) and (22) and Properties 1, 2, we can acquire $\dot{V}_2$ as

$$\begin{aligned}\dot{V}_2 =&\tilde{z}_2^T((\chi(u))u_a + \Delta\tau + W^T\Phi(x) + \epsilon - \tau_{dist})\\ \leq&\tilde{z}_2^T(-z_1 - K_{21}\tilde{z}_2 - K_{22}Sig^{\alpha}(\tilde{z}_2) - K_{23}Sig^{\beta}(\tilde{z}_2)\\ &- \tilde{W}^T\Phi(x) + W^T\Phi(x) + d - Sgn(\tilde{z}_2)\odot\hat{d})\\ \leq&-\sum_{i=1}^{n}(k_{21,i}\tilde{z}_{2,i}^2) - \sum_{i=1}^{n}(k_{22,i}|\tilde{z}_{2,i}|^{\alpha+1}) - \sum_{i=1}^{n}(k_{23,i}|\tilde{z}_{2,i}|^{\beta+1})\\ &+\sum_{i=1}^{n}(|\tilde{z}_{2,i}|d_i) - \sum_{i=1}^{n}(|\tilde{z}_{2,i}|\hat{d}_i) - \tilde{z}_2^T\tilde{z}_1 + \tilde{z}_2^T\tilde{W}^T\Phi(x)\\ \leq&-\sum_{i=1}^{n}(k_{21,i}\tilde{z}_{2,i}^2) - \sum_{i=1}^{n}(k_{22,i}|\tilde{z}_{2,i}|^{\alpha+1}) - \sum_{i=1}^{n}(k_{23,i}|\tilde{z}_{2,i}|^{\beta+1})\\ &+\sum_{i=1}^{n}(|\tilde{z}_i|\tilde{d}_i) - \tilde{z}_2^T\tilde{z}_1 + \tilde{z}_2^T\tilde{W}^T\Phi(x)\end{aligned} \tag{30}$$

Combining (23),(24), (27) and Young's inequality, we can acquire $\dot{V}_3$ as

$$\begin{aligned}\dot{V}_3 =&-\sum_{i=1}^{n}(|\tilde{z}_i|\tilde{d}_i) - \tilde{d}^T\upsilon\hat{d} - tr(\tilde{W}^T(\Phi(x)\tilde{z}_2^T - \lambda\hat{W}))\\ \leq&-\sum_{i=1}^{n}(|\tilde{z}_i|\tilde{d}_i) - \sum_{i=1}^{n}(\frac{\upsilon_i}{2}|\tilde{d}_i|^2) + \sum_{i=1}^{n}(\frac{\upsilon_i}{2}|d_i|^2)\\ &-\tilde{z}_2^T\tilde{W}^T\Phi(x) - \sum_{i=1}^{n}(\frac{\lambda_i}{2}|\tilde{W}_i|^2) + \sum_{i=1}^{n}(\frac{\lambda_i}{2}|W_i|^2)\end{aligned} \tag{31}$$

Step 1: A candidate Lyapunov function V_I is built as:

$$V_I = V_1 + V_2 + V_3 \tag{32}$$

The derivative of V_I is:

$$\begin{aligned}\dot{V}_I =&\dot{V}_1 + \dot{V}_2 + \dot{V}_3\\ \leq&-\sum_{i=1}^{n}(k_{11,i}\tilde{z}_{1,i}^2) - \sum_{i=1}^{n}(k_{21,i}\tilde{z}_{2,i}^2) - \sum_{i=1}^{n}(\frac{\upsilon_i}{2}|\tilde{d}_i|^2)\\ &-\sum_{i=1}^{n}(\frac{\lambda_i}{2}|\tilde{W}_i|^2) + \sum_{i=1}^{n}(\frac{\upsilon_i}{2}|d_i|^2) + \sum_{i=1}^{n}(\frac{\lambda_i}{2}|W_i|^2)\\ =&-aV_I + b\end{aligned} \tag{33}$$

where $b = \sum_{i=1}^{n}(\frac{\upsilon_i}{2}|d_i|^2) + \sum_{i=1}^{n}(\frac{\lambda_i}{2}|W_i|^2) > 0$ and a is also positive constant, which satisfy:

$$a = min(2\lambda_{min}(K_{11}), \frac{2\lambda_{min}(K_{21})}{\lambda_{max}(H)}, \frac{2\lambda_{min}(\lambda)}{\lambda_{max}(\Gamma^{-1})}, 2\lambda_{min}(\upsilon)) \tag{34}$$

where $\lambda_{min}(\cdot)$ and $\lambda_{max}(\cdot)$ denotes the maximum value and the minimum value of diagonal matrix elements.

Following Lemma 1, we can know that if the initial state $V_I(0)$ is guaranteed to be bounded, the related error signals $\psi_s = (\tilde{\xi}_1, \tilde{z}_2, \tilde{W}, \tilde{d})$ that constitute the Lyapunov function V_I are uniformly ultimately bounded(UUB). Therefore,there's some positive constant $\tilde{z}_{1b}$, $\tilde{z}_{2b}$, $\tilde{W}_b$, $\tilde{d}_b$, that makes these inequality $||\tilde{z}_1|| < \tilde{z}_{1b}$, $||\tilde{z}_2|| < \tilde{z}_{2b}$, $||\tilde{W}|| < \tilde{W}_b$, $||\tilde{d}|| < \tilde{d}_b$ always true.

Step 2: We choose another candidate Lyapunov function V_{II}:

$$V_{II} = V_1 + V_2 \tag{35}$$

Taking the derivative of V_{II} :

$$\begin{aligned}\dot{V}_{II} =&\dot{V}_1 + \dot{V}_2\\ \leq&-\sum_{i=1}^{n}(k_{12,i}|\tilde{z}_{1,i}|^{\alpha+1}) - \sum_{i=1}^{n}(k_{13,i}|\tilde{z}_{1,i}|^{\beta+1})\\ &-\sum_{i=1}^{n}(k_{22,i}|\tilde{z}_{2,i}|^{\alpha+1}) + \sum_{i=1}^{n}(k_{23,i}|\tilde{z}_{2,i}|^{\beta+1})\\ &+\sum_{i=1}^{n}(\frac{\upsilon_i}{2}|d_i|^2) + \tilde{z}_2^T\tilde{W}^T\Phi(x)\\ \leq&-\kappa_1 V_{II}^{\frac{\alpha+1}{2}} - \kappa_2 V_{II}^{\frac{\beta+1}{2}} + h\end{aligned} \tag{36}$$

According to the conclusion of the previous step,we have $|\tilde{z}_2^T\tilde{W}^T\Phi(x)| \leq \bar{c}$, where $\bar{c}$ is a positive constant.Then we set h as $h = \bar{c} + \sum_{i=1}^{n}(\frac{\upsilon_i}{2}|d_i|^2)$ .Besides, κ_1, κ_2 satisfy

$$\kappa_1 = min(2\lambda_{min}(K_{12}, 2\lambda_{min}(K_{22}) \tag{37}$$

$$\kappa_2 = min(\frac{2\lambda_{min}(K_{13})n^{\frac{1-\beta}{2}}}{\lambda_{max}(H)}, \frac{2\lambda_{min}(K_{23})n^{\frac{1-\beta}{2}}}{\lambda_{max}(H)}) \tag{38}$$

We can know from Lemma 2 that the correlation signals $\vartheta = (\tilde{z}_1, \tilde{z}_2)$ of the Lyapunov function V_{II} will finally converge to the compact set $\Omega = \left\{\vartheta | V_{II} \leq min\left(\frac{\nu}{\kappa_1(1-\gamma)}^{\frac{2}{\alpha+1}}, \frac{\nu}{\kappa_2(1-\gamma)}^{\frac{2}{\beta+1}}\right)\right\}$ fixed time, where $0 < \gamma < 1$ and the convergence time of the system satisfies: $T \leq T_{max} = \frac{2}{\kappa_1\gamma(1-\alpha)} + \frac{2}{\kappa_2\gamma(\beta-1)}$.

V. Simulation And Results

A. Simulation model

In order to verify the feasibility and effectiveness of the proposed control scheme, a simulation experiment is carried out on the 2-DOF manipulator model [22] . The mass and length parameters of the connecting rod manipulator are $m_1 = 5kg$, $m_2 = 2.5kg$, $g = 9.81N/kg$, $l_1 = 0.6m$, $l_2 = 0.4m$.

During the experiment, the desired trajectory is set as:

$$\theta_d(t) = \begin{bmatrix}\theta_{d1}\\ \theta_{d2}\end{bmatrix} = \begin{bmatrix}-0.5 + 0.8sin(0.8\pi t)\\ -0.3 + 0.8cos(0.8\pi t)\end{bmatrix} \tag{39}$$

The parameters related to input saturation are $\bar{\tau} = [100, 50]^T$, $\bar{u} = [300, 300]^T$, $\upsilon = diag[1, 1]$. The original state is $\theta(0) = [0.5; -0.5]^T$. The gain parameters in the virtual control quantity and control law are $K_{11} = diag[30, 10]$, $K_{12} = diag[5, 3]$, $K_{13} = diag[4, 2]$, $K_{21} = diag[30, 10]$,

$K_{22} = diag[5,3]$, $K_{23} = diag[4,2]$. The parameters of Incremental Broad Neural Network are $\sigma = 50$, $\delta = 0.9$, $m = 3$,$\varepsilon = 12$, $\Gamma = diag[2,2]$, $\lambda = diag[1,1]$.

In order to display the performance of the proposed controller more intuitively, we create a comparison experiment. The comparison controller adopts $PD+$ controll as

$$u = -K_p\tilde{z}_1 - K_d\dot{\tilde{z}}_1 + G$$
$$\tau_i = \begin{cases} \bar{\tau}_i \odot sign(u_i) & ,|u_i| > \bar{\tau}_i \\ u_i & ,|u_i| \leq \bar{\tau}_i \end{cases} \tag{40}$$

where $K_p = diag[150,50]$, $K_d = diag[150,50]$ and gravity G will be compensated completely.

The robustness of the manipulator under disturbance torque needs to be further investigated. A random disturbance torque within the range of $[-5,5]$ and $[-2.5,2.5]$ is set for the first joint and the second respectively.

B. Result analysis

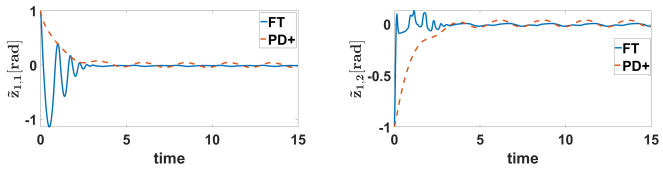

Fig. 3: Tracking errors of θ.

The position tracking errors of the controller is shown in Figure 3, where the solid blue line represents the results of proposed fixed-time controller (FT), and the dotted red line represents the results of PD+ controller. In the transient adjustment process, the joints of the FT controller can converge to the stable state faster than the PD+ controller, and the convergence time is shorter. During the steady-state tracking process, the proposed controller has a stronger tracking ability to the desired trajectory with a smaller steady-state errors. Therefore, it can be concluded that the proposed controller has a good performance in transient regulation and steady state.

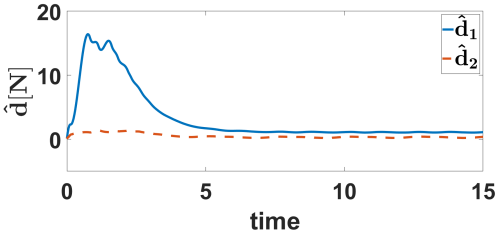

Fig. 4: Estimate of disturbance term d.

A control item $\hat{d}$ is designed to compensate for the error item composed of τ_{dist}, $\Delta\tau$ and ϵ. Figure 4 shows the update of $\hat{d}$ in the tracking process, where the solid blue line corresponds to the first joint and the dotted red line corresponds to the second one. It is not obvious that $\hat{d}$ for both joints can finally converge to constant values, so the designed error compensation control is effective.

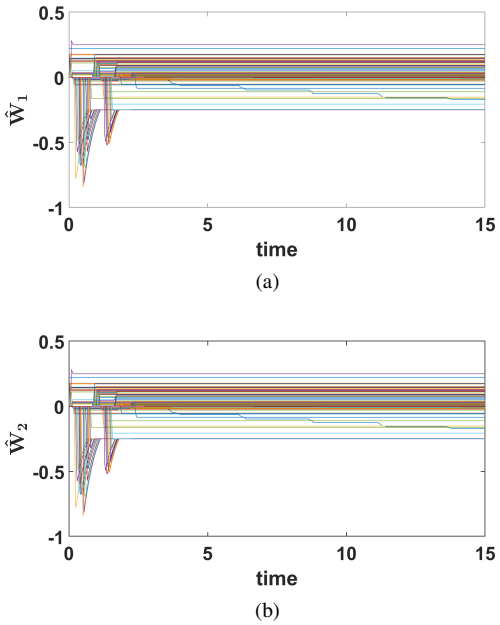

Fig. 5: Weight estimation of IBNN.

Figure 5 shows the weight estimation corresponding to the two joints. The weights of the two joints can converge to the constant values quickly, and the number of activated weights is close to the number of nodes, indicating that the nodes of the neural network are set reasonably and have a good estimation effect of the system uncertainties.

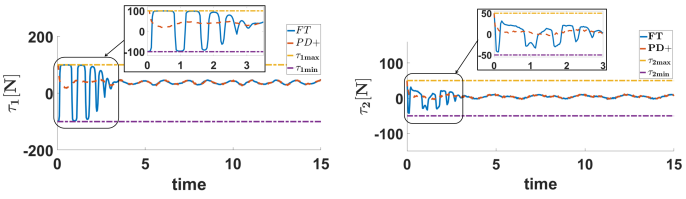

Fig. 6: Actual Control Torque

Figure 6 shows the actual input torque of the controller to the manipulator during the tracking process, where the solid blue line is the result of the proposed controller and the dashed red line is the result of the PD+ controller, and the dotted yellow and purple lines indicate the actuator saturation values. During the whole process, the actual input of both controllers can be within the saturation value range. However, the proposed controller can make full use of the saturation effect, adjust the range of control torque flexibly between the upper and lower saturation values. Although the contrast controller triggered the saturation effect at the beginning, it is attenuated on the whole, leading to the failure that makes full use of the torque range within the saturation interval, which

results in a long adjustment time of the system and a large steady-state error.

TABLE I: Relationship between threshold and precision

parameter	number of nodes	$\tilde{\mathbf{z}}_{\mathbf{1},\mathbf{1}}[\mathbf{rad}]$	$\tilde{\mathbf{z}}_{\mathbf{1},\mathbf{2}}[\mathbf{rad}]$
76	25	0.02780	0.0231
117	18	0.02768	0.0226
191	12	0.02752	0.0222

In order to verify the designed Incremental Broad Neural Network under different approximation performance and control accuracy requirements whether has the characteristics of the flexible adjustment, we set up the horizontal contrast experiment, the experimental results are shown in Table I. In Table I, the 1st column is a distance threshold parameter, the 2nd column is the number of nodes in the network, the 3th and the 4th column is the steady-state error of the two joints. It should be noted that the distance threshold parameter determines the number of nodes in the neural network [19]. The smaller the threshold parameter is, the more nodes there are in the network. It is obvious from the table that the threshold parameter is smaller and the steady-state tracking error of the system is lower. Meanwhile, the convergence time does not increase significantly, indicating that the increase of nodes will not significantly increase the amount of calculation. That is to say, for the higher control accuracy, we only need to simply adjust the distance threshold to ensure the performance requirements and not significantly reduce the computational efficiency.

VI. Conclusion

Aiming at the saturation effect of actuator input and the disturbance of external operating environment of unknown manipulator, we propose an Incremental Broad Neural Network control scheme. By introducing a arctangent function to handle input saturation effect, the control torque input to the actuator can be kept within the saturation value range, and the position tracking errors of the system can converge to stable values in a fixed time. For disturbance torques and uncertainties we build a feedforward control item to compensate the errors. The Incremental Broad Neural Network used to estimate the unknown model of the system has the flexibility of adjustment. For acquring a higher approximation performance and a better tracking effect of the control system , distance threshold parameters need to be simply adjusted, which can guarantee the performance requirements and will not significantly reduce the computational efficiency.

References

[1] S. P. Bhat and D. S. Bernstein, "Lyapunov analysis of finite-time differential equations," in *Proceedings of 1995 American Control Conference-ACC'95*, vol. 3. IEEE, 1995, pp. 1831–1832.

[2] S. P. Bhat and D. S. Bernstein, "Finite-time stability of homogeneous systems," in *Proceedings of the 1997 American control conference (Cat. No. 97CH36041)*, vol. 4. IEEE, 1997, pp. 2513–2514.

[3] V. Andrieu, L. Praly, and A. Astolfi, "Homogeneous approximation, recursive observer design, and output feedback," *SIAM Journal on Control and Optimization*, vol. 47, no. 4, pp. 1814–1850, 2008.

[4] Z. Zuo, Q.-L. Han, B. Ning, X. Ge, and X.-M. Zhang, "An overview of recent advances in fixed-time cooperative control of multiagent systems," *IEEE Transactions on Industrial Informatics*, vol. 14, no. 6, pp. 2322–2334, 2018.

[5] S. Chang, Y. Wang, and Z. Zuo, "Fixed-time active disturbance rejection control and its application to wheeled mobile robots," *IEEE Transactions on Systems, Man, and Cybernetics: Systems*, vol. 51, no. 11, pp. 7120–7130, 2020.

[6] D. Ma, Y. Xia, G. Shen, H. Jiang, and C. Hao, "Practical fixed-time disturbance rejection control for quadrotor attitude tracking," *IEEE Transactions on Industrial Electronics*, vol. 68, no. 8, pp. 7274–7283, 2020.

[7] R. Wei, J. Cao, and J. Kurths, "Fixed-time output synchronization of coupled reaction-diffusion neural networks with delayed output couplings," *IEEE Transactions on Network Science and Engineering*, vol. 8, no. 1, pp. 780–789, 2021.

[8] C. He, J. Wu, J. Dai, Z. Zhe, and T. Tong, "Fixed-time adaptive neural tracking control for a class of uncertain nonlinear pure-feedback systems," *IEEE Access*, vol. 8, pp. 28 867–28 879, 2020.

[9] W. Sun, S. Diao, S.-F. Su, and Z.-Y. Sun, "Fixed-time adaptive neural network control for nonlinear systems with input saturation," *IEEE Transactions on Neural Networks and Learning Systems*, 2021.

[10] Q. Chen, S. Xie, and X. He, "Neural-network-based adaptive singularity-free fixed-time attitude tracking control for spacecrafts," *IEEE Transactions on Cybernetics*, vol. 51, no. 10, pp. 5032–5045, 2020.

[11] N. Li, X. Wu, J. Feng, Y. Xu, and J. Lü, "Fixed-time synchronization of coupled neural networks with discontinuous activation and mismatched parameters," *IEEE Transactions on Neural Networks and Learning Systems*, vol. 32, no. 6, pp. 2470–2482, 2020.

[12] Y. Chu, J. Fei, and S. Hou, "Adaptive global sliding-mode control for dynamic systems using double hidden layer recurrent neural network structure," *IEEE Transactions on Neural Networks and Learning Systems*, vol. 31, no. 4, pp. 1297–1309, 2020.

[13] Z. Lu, N. Wang, and C. Yang, "A novel iterative identification based on the optimised topology for common state monitoring in wireless sensor networks," *International Journal of Systems Science*, vol. 53, no. 1, pp. 25–39, 2022.

[14] X.-N. Shi, Z.-G. Zhou, D. Zhou, and R. Li, "Event-triggered fixed-time adaptive trajectory tracking for a class of uncertain nonlinear systems with input saturation," *IEEE Transactions on Circuits and Systems II: Express Briefs*, vol. 68, no. 3, pp. 983–987, 2020.

[15] C. Yang, D. Huang, W. He, and L. Cheng, "Neural control of robot manipulators with trajectory tracking constraints and input saturation," *IEEE Transactions on Neural Networks and Learning Systems*, vol. 32, no. 9, pp. 4231–4242, 2020.

[16] L. Kong, W. He, W. Yang, Q. Li, and O. Kaynak, "Fuzzy approximation-based finite-time control for a robot with actuator saturation under time-varying constraints of work space," *IEEE Transactions on Cybernetics*, vol. 51, no. 10, pp. 4873–4884, 2020.

[17] C. P. Chen and Z. Liu, "Broad learning system: An effective and efficient incremental learning system without the need for deep architecture," *IEEE transactions on neural networks and learning systems*, vol. 29, no. 1, pp. 10–24, 2017.

[18] Y.-H. Pao, S. M. Phillips, and D. J. Sobajic, "Neural-net computing and the intelligent control of systems," *International Journal of Control*, vol. 56, no. 2, pp. 263–289, 1992.

[19] H. Huang, C. Yang, and S. Dai, "Fixed-time adaptive neural tracking control for robot manipulator with output error constraints," in *2021 International Conference on Security, Pattern Analysis, and Cybernetics (SPAC)*. IEEE, 2021, pp. 120–125.

[20] D. Huang, C. Yang, Y. Pan, and L. Cheng, "Composite learning enhanced neural control for robot manipulator with output error constraints," *IEEE Transactions on Industrial Informatics*, vol. 17, no. 1, pp. 209–218, 2019.

[21] C. Zhu, Y. Jiang, and C. Yang, "Fixed-time neural control of robot manipulator with global stability and guaranteed transient performance," *IEEE Transactions on Industrial Electronics*, 2022.

[22] Y. Jiang, Y. Wang, Z. Miao, J. Na, Z. Zhao, and C. Yang, "Composite-learning-based adaptive neural control for dual-arm robots with relative motion," *IEEE Transactions on Neural Networks and Learning Systems*, 2020.